RSC Advances

PAPER

View Article Online
View Journal | View Issue

Cite this: *RSC Adv.*, 2018, **8**, 26180

8-Hydroxy-2-methylquinoline-modified $H_4SiW_{12}O_{40}$: a reusable heterogeneous catalyst for acetal/ketal formation

Li-jun Liu,[a] Qing-jie Luan,[a] Jing Lu,[a] Dong-mei Lv,[a] Wen-zeng Duan,[a] Xu Wang[b] and Shu-wen Gong *[a]

Received 25th May 2018
Accepted 12th July 2018

DOI: 10.1039/c8ra04471f

rsc.li/rsc-advances

A heteropoly acid based organic hybrid heterogeneous catalyst, HMQ-STW, was prepared by combining 8-hydroxy-2-methylquinoline (HMQ) with Keggin-structured $H_4SiW_{12}O_{40}$ (STW). The catalyst was characterized *via* elemental analysis, X-ray diffractometry (XRD), Fourier transform infrared spectroscopy (FT-IR), scanning electron microscopy (SEM), thermogravimetric analysis (TG) and potentiometric titration analysis. The catalytic performance of the catalyst was assessed in the ketalization of ketones with glycol or 1,2-propylene glycol. Various reaction parameters, such as the glycol to cyclohexanone molar ratio, catalyst dosage, reaction temperature and time, were systematically examined. HMQ-STW exhibited a relatively high yield of corresponding ketal, with 100% selectivity under the optimized reaction conditions. Moreover, catalytic recycling tests demonstrated that the heterogeneous catalyst exhibited high potential for reusability, and it was revealed that the organic modifier HMQ plays an important role in the formation of a heterogeneous system and the improvement of structural stability. These results indicated that the HMQ-STW catalyst is a promising new type of heterogeneous acid catalyst for the ketalization of ketones.

1. Introduction

The formation of acetals/ketals is valuable as a common method for the protection and isolation of carbonyl and polyol compounds.[1] And acetals/ketals are often used as synthetic intermediates, and can be used as starting materials in the production of flavours, disinfectants and surfactants.[1,2] Some glycerol acetals may also find applications as beneficial fuel additives, especially to boost the low temperature properties of biodiesel fuels.[3,4] Mota[5,6] once reported that solketal, when used as a fuel additive, can effectively increase the octane number of gasoline and reduce emissions resulting from fuel combustion.

Acetals and ketals are generally prepared from carbonyl compounds and alcohols in the presence of acid catalysts. Commonly used catalysts generally include sulfuric acid, phosphoric acid, hydrochloric acid and *p*-toluenesulfonic acid.[7,8] Although these homogeneous catalysts have remarkable catalytic activities, corrosion problems are inevitable and the synthetic process can hardly meet requirements to protect the environment. Therefore, it is desirable to investigate solid acid catalysts as an alternative to homogeneous catalysts with the above shortcomings.[9] Several heterogeneous catalysts have been reported for the acetalization and ketalization of different carbonyl compounds, including montmorillonite clay,[7] zeolites,[10] metal(IV) phosphates,[11] activated carbons,[12] acidic resins such as Amberlyst,[13] *etc.* Rat *et al.*[14] once reported a comparison between the catalytic effects of AS-MES (arene sulfonic acid ethane-silica) and AS-SBA-15, indicating that the AS-MES material was more efficient than AS-SBA-15 for the acetalization of heptanal by 1-butanol at 75 °C. Recently, in order to meet the requirements of high activity and environmental protection, new types of catalysts for the formation of acetals and ketals have constantly sprung up.[3,9,15]

As a kind of eco-friendly material, heteropolyacids with a Keggin structure have been widely studied in recent decades. They can be used as a substitute for conventional acid catalysts in acid catalyzed reactions in the liquid phase, owing to their strong Brønsted acidity and uniform acidic sites.[16–19] However, efficient heterogeneous catalysts based on heteropolyacids have to be obtained through "immobilization" or "solidification", since they are highly soluble in polar compounds.[16–20] Supporting heteropolyacids on suitable supports is a useful method for improving the catalytic performance in a heterogeneous reaction, and it also can resolve the problem of the small surface areas (<10 $m^2\ g^{-1}$) of heteropolyacids.[16,21] Ivanov[22] once pointed out that neutral or acidic carriers were more suitable for the preparation of supported heteropolyacid-based catalysts. Therefore, neural alumina was selected to prepare a supported

[a]*Institute of Functional Organic Molecules and Materials, School of Chemistry and Chemical Engineering, Liaocheng University, No. 1 Hunan Road, Liaocheng, 252000, People's Republic of China. E-mail: gongshw@lcu.edu.cn*

[b]*College of Chemistry, Chemical Engineering and Materials Science, Shandong Normal University, Jinan 250014, P. R. China*

tungstophosphoric acid (HPW) catalyst, which was applied to the synthesis of acetals and/or ketals, and the yields of ketals and acetals could reach up to 60.5–86.7%.[23] Ion exchange, *i.e.* the partial or total substitution of H^+ in heteropolyacids with large cation ions such as Cs^+ and Ag^+, is another effective technique in heterogenisation.[24–26] The obtained salts of heteropolyacids are obviously changed from the pore structures of pristine acids, with improved surface area and reusability properties. In addition, co-doped heteropolyacids and mixed salts of heteropolyacids have been developed for acid catalyzed reactions.[27,28] Besides the inorganic cations mentioned above, many organic compounds, such as cyclodextrin, pyridine, 4,4′-bipyridine, aliphatic amines and quaternary ammonium salts, have been utilized to modify heteropolyacids.[29–32] Park[33] prepared 12-phosphotungstic acid-based complex catalysts modified *via* nitrogen-containing heterocycles, including imidazole, pyrazole and 1,2,4-triazole. And these three organic–inorganic hybrid catalysts exhibited good catalytic performance in propylene epoxidation. However, few studies are found to focus on the application of organic–inorganic heterogeneous catalysts in acetalization or ketalization.[32]

In this work, a new organic–inorganic material was prepared through the combination of 8-hydroxy-2-methylquinoline with $H_4SiW_{12}O_{40}$. The material was systematically characterized and its potential was assessed as a heterogeneous catalyst for the synthesis of acetals or ketals. The reaction conditions were optimized and the catalyst reusability was also studied.

2. Experimental

2.1. Materials

Silicotungstic acid ($H_4SiW_{12}O_{40}$, STW, AR), 8-hydroxy-2-methylquinoline (HMQ, AR, 98%), quinaldic acid (QA, AR, >98%), and nicotinic acid N-oxide (NAN, AR, >98%) were purchased from Energy Chemical Co., Ltd. All other organic reagents were of analytical grade and used as received without further purification.

2.2. Material preparation

The preparation of HMQ modified STW was carried out in aqueous solution. In a typical procedure, STW (0.001 mol, 2.878 g) was dissolved in 20 mL of distilled water with vigorous stirring at 50 °C. Then HMQ solution (0.004 mol, 0.636 g, 0.4 mol L^{-1}) was added dropwise, and the resulting solution was kept under stirring conditions for over 12 h at 50 °C. The resulting green-yellow precipitate was filtered and dried at 100 °C to obtain the final modified catalyst (HMQ-STW).

Meanwhile, the other control materials were synthesized, changing HMQ to QA or NAN. The obtained catalysts were named QA-STW and NAN-STW, respectively.

2.3. Characterization

Elemental analysis (C, H and N) was performed using a PerkinElmer 2400 elemental analyzer.

The XRD patterns of the catalyst were obtained using a XD-3 diffractometer (Beijing Purkinje General Instrument Co. Ltd.) with Cu K_α (1.542 Å) radiation at a scanning rate of 4° min^{-1} over a 2θ range from 5° to 50°.

FT-IR spectra were scanned using a Thermo Nicolet 6700 FT-IR spectrometer using the KBr disc technique (4000–400 cm^{-1}).

UV-vis absorption spectra were recorded using a T9CS UV-vis spectrophotometer (Persee Instrument Co., Ltd. Beijing, China), using a matched pair of quartz cells with a 1 cm path length. Ethanol was used as the background.

Thermogravimetric (TG) analysis was performed on a PerkinElmer-7 instrument at a heating rate of 5 °C min^{-1}.

Scanning electron microscopy (SEM) images were obtained using a JSM6380LV type scanning electron microscope.

The mean pore diameter and pore volume of HMQ-STW were determined *via* N_2 adsorption–desorption techniques performed at −196 °C using a Quantachrome Autosorb IQ-C instrument. Before measurements, samples were evacuated at 200 °C for 2 h.

The potentiometric titration method was used to test the acidity of the solid samples through an automatic potentiometric titrator with a pH composite electrode.[34,35] The catalyst (0.05 g) was suspended in 15 mL of methanol and stirred for 2 h at room temperature. The turbid liquid was titrated with a solution of 0.05 mol L^{-1} *n*-butylamine in acetonitrile.

2.4. Catalytic tests

The catalytic properties of the catalyst were studied for the ketalization of glycol by cyclohexanone. The reaction was carried out in a three-neck flask equipped with a magnetic stirrer, a reflux condenser and Dean–Stark apparatus. In a typical procedure, certain amounts of cyclohexanone, glycol, cyclohexane and catalyst were mixed, where cyclohexane was the water-carrying agent. Under vigorous stirring, the reaction mixture was heated at different reaction temperatures (75 °C, 85 °C, 95 °C, 105 °C and 115 °C) over a certain time. Upon completion, the catalytic system was cooled down to room temperature immediately, and the catalyst was separated from the reaction mixture *via* filtration. The composition of the products was identified using gas chromatography-mass spectrometry (GC-MS, HP-5MS UI capillary column, 30 m × 0.25 mm, 0.25 μm film thickness).

3. Results and discussion

3.1. Characterization

3.1.1. XRD analysis and elemental analysis of the catalyst. XRD patterns of the prepared HMQ-STW catalyst and the raw materials are presented in Fig. 1. For STW, the main diffraction peaks that appeared at 7.9°, 9.1°, 21.3°, 25.7°, 27.4° and 36.0° can be assigned to the crystalline STW Keggin structure.[36] HMQ showed the main diffraction peaks at approximately 11.1°, 16.4° and 22.4°, which indicates that HMQ exhibited a highly crystalline structure. In the case of HMQ-STW, some diffraction peaks similar to STW were observed, and these peaks also appeared in the four regions 7–10°, 15–21°, 26–30° and 35–38°, so they may be still attributed to the characteristic peaks of the Keggin structure of raw STW. Otherwise, the most intense

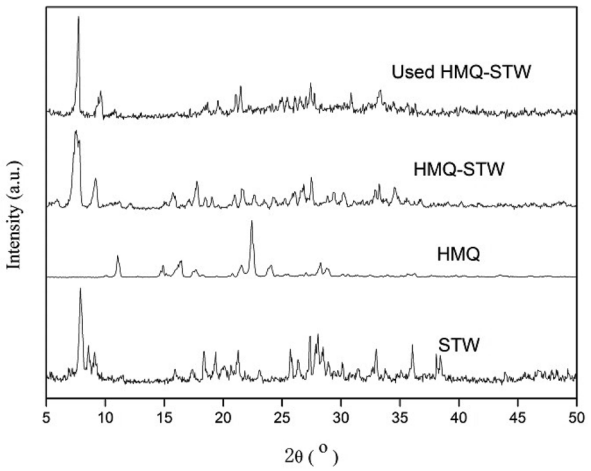

Fig. 1 XRD patterns of pristine STW, HMQ, HMQ-STW and used HMQ-STW.

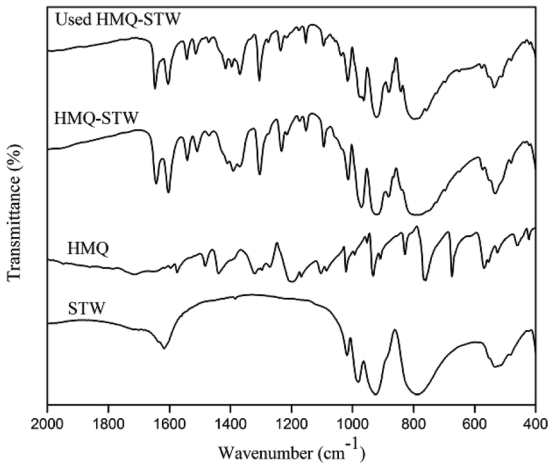

Fig. 2 FT-IR spectra of pristine STW, HMQ, HMQ-STW and used HMQ-STW.

diffraction peak of STW at 7.9° is slightly shifted to a lower 2θ value and emerges at 7.5° for HMQ-STW. In addition, the two peaks at 28.0° and 36.0° of STW were not observed in the pattern of HMQ-STW. This result indicates that HMQ-STW showed a diffractive pattern different from those of STW and HMQ, and the pattern was not a simple superposition of those of the two raw materials, which meant that a new crystalline phase formed through the combination of STW and HMQ in aqueous solution.

Elemental analysis (C, H and N) of an HMQ-STW sample was performed to confirm the element content. The analysis results show 13.35% as the weight percentage of C, with 1.53% for N and 1.18% for H; these are close to the calculated values of C, 13.67%, N, 1.59%, and H, 1.15%, according to the used amounts of HMQ and STW. Therefore, it could be preliminarily speculated that the theoretical formula of HMQ-STW is $[(C_{10}H_9NO)]_4H_4SiW_{12}O_{40}$.

3.1.2. FT-IR analysis of the catalyst. FT-IR spectra of the prepared HMQ-STW catalyst and raw materials are presented in Fig. 2. The spectrum of pristine STW shows a characteristic Keggin structure, with bands at 1018 cm^{-1} (Si–O), 981 cm^{-1} (W = O_t), 924 cm^{-1} (Si–O), 884 cm^{-1} (W–O_c–W) and 790 cm^{-1} (W–O_e–W).[16,37] These characteristic bands (1014, 970, 920, 881 and 788) were also found in the spectrum of HMQ-STW, indicating that the Keggin structure of STW was maintained in the HMQ-STW catalyst. However, these peaks shift slightly, implying a slight distortion of the Keggin STW framework. That might be caused by the extension of the conjugated electrons of organic cations to STW anions.[38] Some bands attributed to HMQ were observed in the range of 1600–1100 cm^{-1}. The absorption peaks at 1510 cm^{-1} and 1470 cm^{-1} could be related to the quinoline ring, indicating that HMQ was successfully connected with STW. It was worth noting that there were two new bands at 1643 cm^{-1} and 1541 cm^{-1} in the spectrum of HMQ-STW. The former could be related to the stretching vibration of C=N and C=C bonds in HMQ-STW heterocycles.[39] The latter could be related to the protonated quinolone ring, which was based on the fact that this band has often been ascribed to the chemisorption of pyridine on Brønsted acid centers and that there is similarity between nitrogen atoms in quinoline rings and pyridine rings.[38] These observations not only revealed the coexistence of HMQ and Keggin-structured $SiW_{12}O_{40}^{4-}$ anions in HMQ-STW, but also illustrated the existence of electronic interaction between the metal oxygen clusters in the anions and HMQ. So it could be tentatively proposed that the combination of protonated HMQ as a cation with the $SiW_{12}O_{40}^{4-}$ anion produces a new organic STW salt family.

3.1.3. UV-vis analysis of the catalyst. Fig. 3 shows UV-vis absorption spectra of STW, HMQ and HMQ-STW. The characteristic band at 265 nm of STW could be attributed to an oxygen-to-metal charge transfer band ($O^{2-} \rightarrow W^{6+}$) that presents in the $[SiW_{12}O_{40}]^{4-}$ anion.[40,41] For HMQ-STW, the characteristic band shifted to a lower wavelength and appeared at 259 nm, indicating that STW interacts with HMQ and there is electronic interaction between the Keggin units and HMQ. This result further supports the analysis from FT-IR.

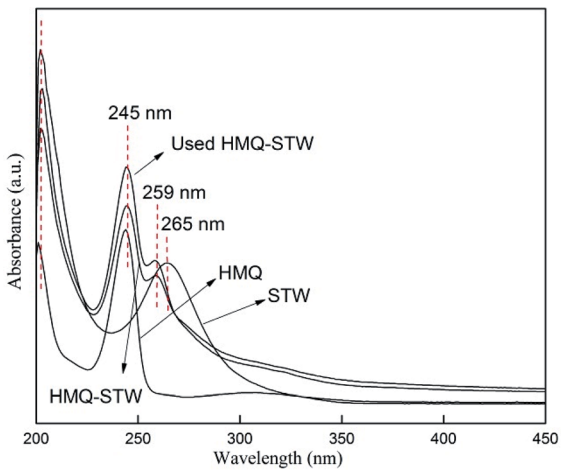

Fig. 3 UV-vis spectra of STW, HMQ, HMQ-STW and used HMQ-STW.

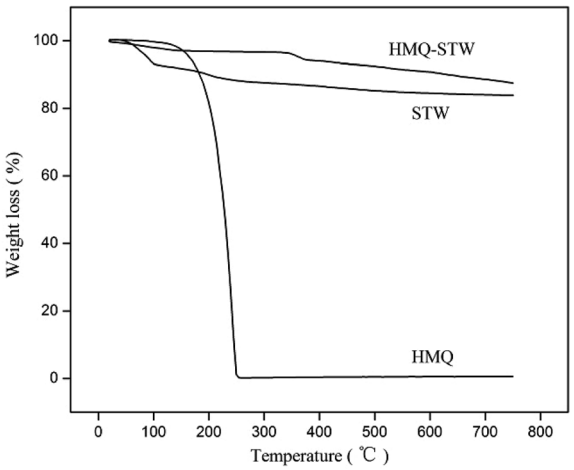

Fig. 4 TG curves of HMQ, STW and HMQ-STW.

3.1.4. TG analysis of the catalyst. The thermal stability of STW, HMQ and the prepared HMQ-STW catalyst were investigated *via* thermogravimetric (TG) analysis, as shown in Fig. 4. For STW, a weight loss of about 8% occurred from room temperature to 90 °C, owing to the removal of free water on the surface of the sample. The second stage, with about 5% weight loss, occurred from 90 °C to 270 °C, accounting for the water of hydration of STW.[41,42] Following this was slow weight loss corresponding to the decomposition of the Keggin anion, which often occurs in the temperature range of 350–600 °C.[42] HMQ only showed a sharp degradation with complete weight loss between 120 and 250 °C. The first mass loss of HMQ-STW occurred from room temperature to 150 °C, accounting for about 3%, owing to the removal of physically adsorbed water. The second mass loss occurred between 330 °C to 380 °C and was followed by slow weight loss that was similar to that of bulk STW. In the temperature range of 150–330 °C, HMQ-STW showed little weight loss; in particular, sharp degradation similar to HMQ was not found. These results further confirmed the combination of HMQ and STW. The combination can enhance the thermal stability of the raw materials, and the second mass loss of HMQ-STW may indicate that the combination of STW and HMQ is starting to be destroyed. Accordingly, HMQ-STW has thermal stability up to 330 °C, indicating that it can be a desirable catalyst in acetalization or ketalization reactions.

3.1.5. SEM analysis of the catalyst. The surface morphologies of pristine STW and the HMQ-STW catalyst are illustrated through SEM micrographs, as presented in Fig. 5. Large agglomerates with irregular block structures were found for pristine STW and the size of these particles was about 100 μm. However, HMQ-STW showed complete different morphology from bulk STW. Most of the HMQ-STW particles appeared in the shape of rice or plates, and their mean size was less than 10 μm, indicating that the combination of HMQ and STW caused a change in morphology. The N_2 adsorption–desorption results showed that the mean pore diameter and the pore volume of STW were 3.716 nm and 0.016 $cm^3\ g^{-1}$, while those of HMQ-STW were 1.753 nm and 0.013 $cm^3\ g^{-1}$, respectively. These results indicated that the combination of STW and HMQ had no improving effects on the textural properties.

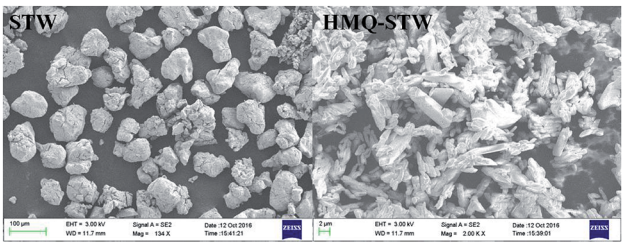

Fig. 5 SEM images of STW and HMQ-STW.

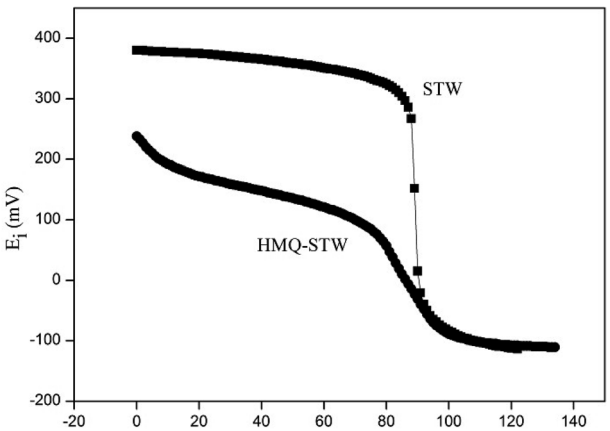

Fig. 6 Potentiometric titration curves for STW and HMQ-STW.

3.1.6. Potentiometric titration of the catalyst. The acid strength of HMQ-STW was evaluated by means of potentiometric titration with *n*-butylamine (Fig. 6). As criteria to interpret the obtained results, it was suggested that the initial electrode potential (E_i) indicates the maximum acid strength of the sites and the volume of solution of *n*-butylamine in acetonitrile where a plateau is reached indicates the total number of acid sites. Since a high initial potential (380 mV) was observed, bulk STW has very strong acidity, which is consistent with results reported in the literature.[43] For HMQ-STW, the initial potential (238 mV) was lower than that of bulk STW, indicating that the combination of HMQ and STW resulted in a decrease in acidity. However, HMQ-STW can still be classified as a strong acid based on the classification criteria.[34,35] The lower acid strength of the HMQ-STW sample compared to bulk STW could be attributed to the fact that STW can be completely dissolved in methanol, while HMQ-STW cannot. In addition, the decrease in acidity may also result from the replacement of protons in STW by protonated HMQ species.

3.2. Catalytic activity

The reaction of cyclohexanone with glycol in the presence of the HMQ-STW catalyst was chosen as a model reaction of ketal formation. Parallel tests were performed using several control samples, including STW, HMQ, NAN-STW and QA-STW, under

Table 1 Catalytic performance of different catalysts in the ketalation of cyclohexanone with glycol

Catalyst	Catalyst solubility in the reaction	Potentiometric titration (E_i)	Yield[a] (%)
None			38.2
HMQ	Soluble	150	40.5
STW	Soluble	380	99.1
HMQ-STW	Insoluble	238	96.0
NAN-STW	Soluble	376	98.6
QA-STW	Soluble	352	97.7

[a] Reaction conditions: catalyst content = 7 wt% of cyclohexanone; mole ratio of glycol to cyclohexanone = 3 : 1; reaction temperature = 105 °C; reaction time = 60 min; 5 mL of cyclohexane.

the same conditions as for HMQ-STW (Table 1). It was shown that the yield of cyclohexanone glycol ketal was only 38.2% in the absence of catalyst, and the ketal was the uniquely detected product. HMQ gave a low yield near to that of the blank experiment, indicating that HMQ has extremely low catalytic activity. In contrast, a high yield of 99.1% was obtained when STW was used as a catalyst. Nonetheless, HMQ and STW were homogeneous samples due to their good solubility in the reaction media. The yield of the modified sample, HMQ-STW, was 96.0%, which was slightly lower than that of pure STW. However, its advantage was that it was not a homogeneous catalyst any longer, which will simplify the recycling process for this catalyst. For the other two modified catalyst, NAN-STW and QA-STW, although they exhibited high catalytic activity with strong acidity, they were still homogeneous catalysts in the model reaction. So, HMQ-STW was selected as a heterogeneous catalyst to systematically study the catalytic performance under different conditions.

3.2.1. Effects of catalyst dosage. The reaction of cyclohexanone with glycol was performed with different dosages of HMQ-STW catalyst (0, 1, 3, 5, 7, and 9 wt% of cyclohexanone) under the conditions of a glycol/cyclohexanone ratio of 3 : 1 for 60 min at 105 °C with 5 mL of the water-carrying agent cyclohexane. As shown in Fig. 7a, the yield of ketal significantly increased with the addition of catalyst into the reaction system and a yield of 75.5% was obtained when the catalyst dosage was only 1 wt% (based on the quantity of cyclohexanone), which further indicated that HMQ-STW has excellent catalytic activity. With an increase in the catalyst dosage from 1 wt% to 7 wt%, the yield increased slightly and eventually reached 96.0% with a catalyst dosage of 7 wt%. However, the conversion decreased when the catalyst dosage increased to above 9 wt%, which may be related to excess catalyst resulting in the higher availability of active sites, which may facilitate the reverse reaction.[44] Therefore, 7 wt% was chosen as the optimum catalyst dosage and was used for further investigation in the present research.

3.2.2. Effects of reaction time. The reaction of cyclohexanone and glycol with 7 wt% HMQ-STW as catalyst was performed over different durations ranging from 40 min to 80 min to study the effects of the reaction time on the synthesis of cyclohexanone glycol ketal. As shown in Fig. 7b, with an extension of the reaction time (40 min to 60 min), the yield of

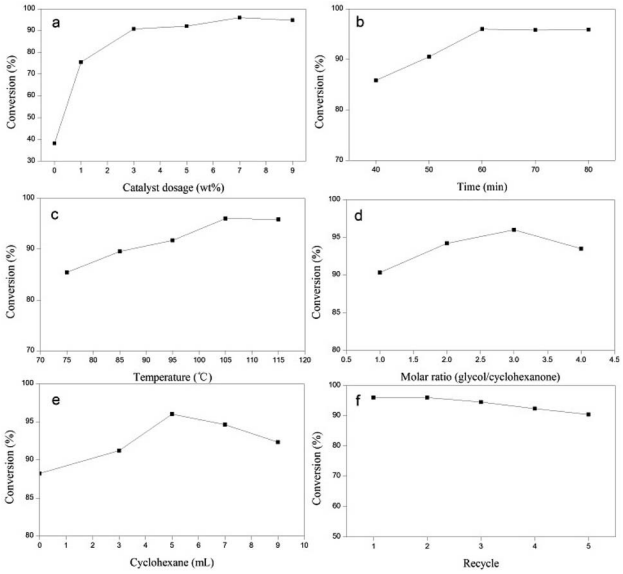

Fig. 7 Effects of reaction parameters on the ketalization of cyclohexanone and glycol: (a) catalyst dosage; (b) reaction time; (c) reaction temperature; (d) molar ratio of glycol to cyclohexanone; (e) amount of water-carrying agent; and (f) catalyst recycling. Reaction conditions: (a) 0.02 mol of cyclohexanone, 7 wt% catalyst, 5 mL of cyclohexane, 60 min, 105 °C; (b) 0.02 mol of cyclohexanone, 0.06 mol of glycol, 7 wt% catalyst, 5 mL of cyclohexane, 105 °C; (c) 0.02 mol of cyclohexanone, 0.06 mol of glycol, 5 mL of cyclohexane, 60 min, 105 °C; (d) 0.02 mol of cyclohexanone, 0.06 mol of glycol, 7 wt% catalyst, 5 mL of cyclohexane, 60 min; (e) 0.02 mol of cyclohexanone, 0.06 mol of glycol, 7 wt% catalyst, 105 °C, 60 min; and (f) 0.02 mol of cyclohexanone, 0.06 mol of glycol, 7 wt% catalyst, 5 mL of cyclohexane, 105 °C, 60 min.

ketal increased, which suggested that allowing a sufficient reaction time was crucial to obtain a high yield. However, as the reaction time was further prolonged to 70 or 80 min, the yield remained stable, probably due to ketalization being reversible. Reversible ketalization may easily take place when the reaction time was longer than 60 min. The results indicated that the optimum reaction time under the conditions of this experiment was 60 min.

3.2.3. Effects of reaction temperature. Fig. 7c plots the effects of reaction temperature on the yield of the ketal over the HMQ-STW catalyst. It shows that an increase in reaction temperature from 70 °C to 105 °C could enhance the yield of ketal, indicating that a higher temperature was conducive to the synthesis of ketal over the evaluated temperature region. The maximum yield of 96.0% was obtained at 105 °C and it hardly changed when the reaction was further heated up to 115 °C, which may be due to the fact that acetal/ketal formation is reversible and it could be beneficial to the reverse reaction when the temperature is higher than 105 °C. So 105 °C should be a suitable reaction temperature.

3.2.4. Effects of the glycol to cyclohexanone molar ratio. Ketalization is usually carried out in the case of excessive alcohol to ensure that the reaction will take place in the direction of ketal synthesis. Fig. 7d shows the impact of the molar ratio of glycol to cyclohexanone on the synthesis of cyclohexanone glycol ketal. A higher yield of 90.3% was obtained when

Table 2 Ketalization of carbonyl compounds with diols catalyzed with HMQ-STW

Entry	Ketone/aldehyde	Diol	Product	Yield[a]/%
1	Benzaldehyde	Glycol	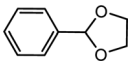	97.7
2	Acetophenone	Glycol	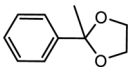	94.3
3	*p*-Nitrobenzaldehyde	Glycol	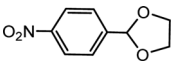	100
4	*m*-Nitrobenzaldehyde	Glycol	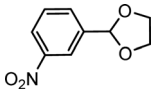	98.6
5	*p*-Chlorobenzaldehyde	Glycol	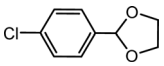	99.5
6	*p*-Nitroacetophenone	Glycol	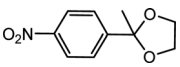	100
7	Benzaldehyde	1,2-Propylene glycol	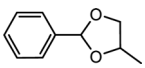	99.7
8	Acetophenone	1,2-Propylene glycol	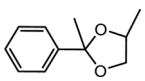	91.3
9	Cyclohexanone	1,2-Propylene glycol	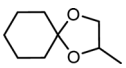	94.6
10	*p*-Chlorobenzaldehyde	1,2-Propylene glycol	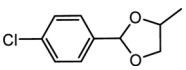	98.6
11	*p*-Nitrobenzaldehyde	1,2-Propylene glycol	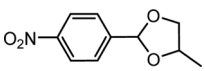	100
12	*p*-Nitroacetophenone	1,2-Propylene glycol	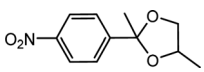	100
13	Acetone	1,2-Propylene glycol	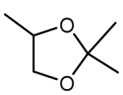	100
14 (ref. 45)	Benzaldehyde	Glycol	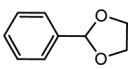	85.0[b]
15 (ref. 46)	Benzaldehyde	Pentaerythritol		92.0[c]
16 (ref. 47)	Benzaldehyde	Neopentyl glycol	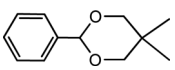	95.0[d]

[a] Reaction conditions: catalyst content = 7 wt% of ketone; mole ratio of diol to ketone = 3 : 1; reaction temperature = 105 °C; reaction time = 60 min; 5 mL of cyclohexane. [b] Amount of $[PPSH]_{2.0}HPW_{12}O_{40}$ catalyst = 5 wt%; glycol/benzaldehyde ratio = 1.8; 12 mL of cyclohexane; reflux reaction for 3 h. [c] Amount of 15 wt% PW/MCM-41 catalyst = 0.3 g; pentaerythritol/benzaldehyde ratio = 1 : 3; 20 mL of toluene/benzene; reflux reaction for 2 h. [d] Amount of $Fe(HSO_4)_3$ catalyst = 8 mol%; neopentyl glycol/benzaldehyde ratio = 1.2 : 1; 3 mL of anhydrous CH_2Cl_2; reflux reaction for 45 min.

the molar ratio of glycol to cyclohexanone was only 1 : 1, which indicated that HMQ-STW has the advantage of obtaining a high yield even at a lower molar ratio of glycol to cyclohexanone. With the molar ratio increasing to 3 : 1, the yield slightly increased to 96.0%. However, higher ratios (*e.g.* 4 : 1) were found to negatively influence the reaction, which could possibly be attributed to insufficient mixing of the reactants with the heterogeneous catalyst when there was a lot of excessive glycol, as well as there being a decrease in catalyst concentration. Therefore, in order to obtain a high yield, the optimum molar ratio of glycol to cyclohexanone for this system was 3 : 1.

3.2.5. Effects of water-carrier dosage. The presence of water could cause the hydrolysis of ketals, so cyclohexane was selected as a water-carrying agent to remove water from the system. Fig. 7e illustrates the impact of the dosage of cyclohexane on the synthesis of cyclohexanone glycol ketal. With the addition of

cyclohexane, the yield of ketal increased significantly, indicating that cyclohexane could effectively remove water from the reaction system. When the amount of cyclohexane was 5 mL, the yield of ketal reached its maximum value (96.0%). However, the yield decreased as the amount of cyclohexane continued to increase. Therefore, the optimum dosage of cyclohexane was 5 mL under these experimental conditions.

3.2.6. Catalyst reusability. After the reaction, the HMQ-STW catalyst was recovered through filtration, washed with distilled water, dried at 100 °C and then reused. As shown in Fig. 7f, when the catalyst was continuously used over five cycles under the above-mentioned optimal conditions, the yield decreased by 6%. After five runs, the catalyst was collected and characterized *via* XRD, FT-IR and UV-vis. As shown in Fig. 1, the main XRD peaks of the catalyst before and after use were almost identical, indicating that there were no obvious changes in the catalyst structure after ketalization. Similarly, the spent catalyst presented a similar IR spectrum to fresh HMQ-STW, proving that the fine structure, including the Keggin unit structure, was not damaged during the reaction (Fig. 2). A UV-vis spectrum of the used catalyst showed charge transfer absorption bands similar to those seen for fresh HMQ-STW, implying that the interaction between STW and HMQ was not significantly affected during the progress of the reaction (Fig. 3). These results demonstrated the good stability of the HMQ-STW catalyst in the reaction of cyclohexanone with glycol.

3.3. Catalytic performance of HMQ-STW for other ketalization reactions

Since HMQ-STW had superior catalytic activity for the reaction of cyclohexanone with glycol, reactions with other substrates (Table 2) were attempted to evaluate the application of HMQ-STW. The results were inspiring. When benzaldehyde and acetophenone were respectively subjected to ketalization with glycol, high yields of the corresponding ketals were obtained as well (entries 1–2). Furthermore, the yields were even higher when there was an electron withdrawing group, such as nitro-, in the benzene ring of the aromatic aldehydes and ketones (entries 3–6). For studying the effects of diol variation, glycol was substituted with 1,2-propylene glycol (entries 7–13). High yields still were obtained for all the ketones used in these experiments. And it was worth pointing out that ketals were the only product, attesting to high selectivity in all these reactions. These results demonstrated that the HMQ-STW catalyst is a suitable catalyst for ketalization and has great potential for the catalytic synthesis of many types of ketals.

Compared with reported catalysts, including heteropolyacid-based ionic liquids and supported heteropolyacids (entries 14–16), HMQ-STW exhibited comparable catalytic activity under similar reaction conditions in the formation of acetals/ketals.

4. Conclusions

In summary, the facile synthesis of a novel organic salt of $H_4SiW_{12}O_{40}$ with a Keggin structure was described in this paper. This material displayed excellent catalytic performance in the preparation of ketals from ketones with glycol or 1,2-propylene glycol. In all the reactions, not only could a high yield of the corresponding ketal be obtained, but HMQ-STW also exhibited excellent reusability and stability. The catalyst could be easily recycled *via* filtration, and its fine structure, including the Keggin unit structure, was not damaged during the reaction. Therefore, HMQ-STW was a promising catalyst for the ketalization reaction, and it can be preliminarily forecast that the catalyst will have potential for future development as an environmentally friendly heterogeneous solid acid catalyst.

Conflicts of interest

There are no conflicts to declare.

Acknowledgements

The authors are grateful for the support of the Shandong Provincial Natural Science Foundation, China (ZR2017MB060, ZR2017MB052), the National Natural Science Foundation of China (21101086) and the Foundation of Liaocheng University (318011406).

References

1 K. Sato, T. Kishimoto, M. Morimoto, H. Saimotob and Y. Shigemasa, *Tetrahedron Lett.*, 2003, **44**, 8623–8625.
2 V. Kannan, K. Sreekumar, A. Gil and M. A. Vicente, *Catal. Lett.*, 2011, **141**, 1118–1122.
3 M. R. Nanda, Y. Zhang, Z. Yuan, W. Qin, H. S. Ghaziaskar and C. B. (C.) Xu, *Renewable Sustainable Energy Rev.*, 2016, **56**, 1022–1031.
4 G. Chen, Y. Li, W. Zhao, K. Qu, Y. Ning and J. Zhang, *Fuel Process. Technol.*, 2015, **133**, 64–68.
5 P. H. R. Silva, V. L. C. Gonçalves and C. J. A. Mota, *Bioresour. Technol.*, 2010, **101**, 6225–6229.
6 C. J. A. Mota, C. X. A. da Silva, N. Rosenbach Jr, J. Costa and F. da Silva, *Energy Fuels*, 2010, **24**, 2733–2736.
7 M. N. Timofeeva, V. N. Panchenko, V. V. Krupskaya, A. Gil and M. A. Vicente, *Catal. Commun.*, 2017, **90**, 65–69.
8 M. Gonçalves, R. Rodrigues, T. S. Galhardo and W. A. Carvalho, *Fuel*, 2016, **181**, 46–54.
9 A. R. Trifoi, P. Ş. Agachi and T. Pap, *Renewable Sustainable Energy Rev.*, 2016, **62**, 804–814.
10 J. Kowalska-Kus, A. Held, M. Frankowski and K. Nowinska, *J. Mol. Catal. A: Chem.*, 2017, **426**, 205–212.
11 S. M. Patel, U. V. Chudasama and P. A. Ganeshpure, *J. Mol. Catal. A: Chem.*, 2003, **194**, 267–271.
12 R. Rodrigues, M. Goncalves, D. Mandelli, P. P. Pescarmona and W. A. Carvalho, *Catal. Sci. Technol.*, 2014, **4**, 2293–2301.
13 J. Deutsch, A. Martin and H. Lieske, *J. Catal.*, 2007, **245**, 428–435.
14 M. Rat, M. H. Zahedi-Niaki, S. Kaliaguine and T. O. Do, *Microporous Mesoporous Mater.*, 2008, **112**, 26–31.
15 L. Chen, B. Nohair and S. Kaliaguine, *Appl. Catal., A*, 2016, **509**, 143–152.

16 L. C. Liu, B. Wang, Y. Y. Du and A. Borgna, *Appl. Catal., A*, 2015, **489**, 32–41.
17 W. H. Zhang, Y. Leng, D. R. Zhu, Y. J. Wu and J. Wang, *Catal. Commun.*, 2009, **11**, 151–154.
18 Y. Leng, J. Wang, D. R. Zhu, X. Q. Ren, H. Q Ge and L. Shen, *Angew. Chem., Int. Ed.*, 2009, **48**, 168–171.
19 Y. Zhou, G. J. Chen, Z. Y. Long and J. Wang, *RSC Adv.*, 2014, **4**, 42092–42113.
20 J. Li, D. F. Li, J. Y. Xie, Y. Q. Liu, Z. J. Guo, Q. Wang, Y. Lyu, Y. Zhou and J. Wang, *J. Catal.*, 2016, **339**, 123–134.
21 S. K. Bhorodwaj and D. K. Dutta, *Appl. Catal., A*, 2010, **378**, 221–226.
22 A. V. Ivanov, T. V. Vasina and V. D. Nissenbaum, *Appl. Catal., A*, 2004, **259**, 65–72.
23 J. Z. Gao, Y. X. Wei, X. M. Wang and W. Yang, *Rare Met.*, 2007, **26**, 152–157.
24 K. M. Parida, S. Rana, S. Mallick and D. Rath, *J. Colloid Interface Sci.*, 2010, **350**, 132–139.
25 S. H. Zhu, X. Q. Gao, F. Dong, Y. L. Zhu, H. Y. Zheng and Y. W. Li, *J. Catal.*, 2013, **306**, 155–163.
26 M. Safariamin, S. Paul, K. Moonen, D. Ulrichts, F. Dumeignil and B. Katryniok, *Catal. Sci. Technol.*, 2016, **6**, 2129–2135.
27 Q. Y. Zhang, F. F. Wei, Q. Li, J. S. Huang, Y. M. Fenga and Y. T. Zhang, *RSC Adv.*, 2017, **7**, 51090–51095.
28 J. S. Santos, J. A. Dias, S. C. L. Dias, J. L. de Macedo, F. A. C. Garcia, L. S. Almeida and E. N. C. B. de Carvalho, *Appl. Catal., A*, 2012, **443–444**, 33–39.
29 In K. Song, M. S. Kaba and M. A. Barteau, *J. Phys. Chem.*, 1996, **100**, 17528–17534.
30 Z. Y. Long, Y. Zhou, G. J. Chen, P. P. Zhao and J. Wang, *Chem. Eng. J.*, 2014, **239**, 19–25.
31 H. Ge, Y. Leng, F. M. Zhang, C. J. Zhou and J. Wang, *Catal. Lett.*, 2008, **124**, 250–255.
32 S. Sandesh, A. B. Halgeri and G. V. Shanbhag, *J. Mol. Catal. A: Chem.*, 2015, **401**, 73–80.
33 H. J. Kim, Y. Jeon, J.-I. Park and Y.-G. Shul, *J. Mol. Catal. A: Chem.*, 2013, **378**, 232–237.
34 R. Cid and G. Pecchi, *Appl. Catal.*, 1985, **14**, 15–21.
35 L. R. Pizzio, P. G. Vázquez, C. V. Cáceres and M. N. Blanco, *Appl. Catal., A*, 2003, **256**, 125–139.
36 G. F. Chen, J. Li, X. G. Yang and Y. Wu, *Appl. Catal., A*, 2006, **310**, 16–23.
37 K. Yan, G. S. Wu, J. L. Wen and A. C. Chen, *Catal. Commun.*, 2013, **34**, 58–63.
38 L. S. Felices, P. Vitoria, J. M. Gutiérrez-Zorrilla, S. Reinoso, J. Etxebarria and L. Lezama, *Chem.–Eur. J.*, 2004, **10**, 5138–5146.
39 Z. Y. Long, G. J. Chen, S. Liu, F. M. Huang, L. M. Sun, Z. L. Qin, Q. Wang, Y. Zhou and J. Wang, *Chem. Eng. J.*, 2018, **334**, 873–881.
40 J. Gong, X. J. Cui, Z. W. Xie, S. G. Wang and L. Y. Qu, *Synth. Met.*, 2002, **129**, 187–192.
41 S. Shanmugam, B. Viswanathan and T. K. Varadarajan, *J. Membr. Sci.*, 2006, **275**, 105–109.
42 Y. H. Kong, X. M. Cheng, H. L. An, X. Q. Zhao and Y. J. Wang, *Chin. J. Chem. Eng.*, 2018, **26**, 330–336.
43 I. V. Kozhevnikov, *Chem. Rev.*, 1998, **98**, 171–198.
44 A. N. Chermahini and M. Nazeri, *Fuel Process. Technol.*, 2017, **167**, 442–450.
45 X. X. Han, W. Yan, K. K. Chen, C. T. Hung, L. L. Liu, P. H. Wu, S. J. Huang and S. B. Liu, *Appl. Catal., A*, 2014, **485**, 149–156.
46 B. R. Jermy and A. Pandurangan, *Appl. Catal., A*, 2005, **295**, 185–192.
47 H. Eshghi, M. Rahimizadeh and S. Saberi, *Catal. Commun.*, 2008, **9**, 2460–2466.